Date File S2
Microremain identification criteria supplement for
Early evidence for long-distance trade in exotic foods and spices from South Asia to the Near East in the 2nd millennium BCE

Ashley Scott, Robert C. Power, Victoria Altmann-Wendling, Michal Artzy, Mario A. S. Martin, Stefanie Eisenmann, Richard Hagan, Domingo Carlos Salazar García, Yossi Salmon, Dmitry Yegorov, Ianir Milevski, Israel Finkelstein, Philipp W. Stockhammer, Christina Warinner

Unspecific parts of grass phytoliths

Morphotypes used for identification: hairs, short-cells

Source: (Piperno, 2006; Twiss et al., 1969)

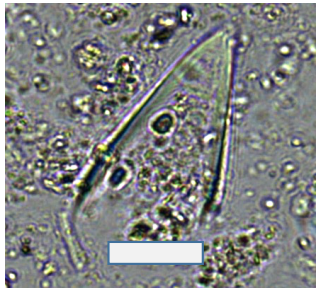

Hair phytolith in MGD011.
Scale bar is 20 microns.

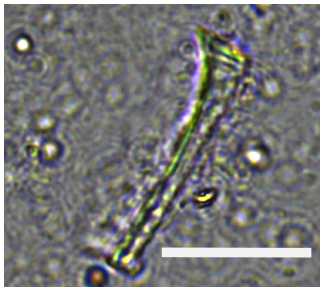

Trapezoid phytolith in MGD011.
Scale bar is 20 microns.

Grass/cereals leaves and grass stem phytoliths

Morphotypes used for identification: long-cell wavy, long-cell polylobate, parallelepiped thin smooth, blocky bulliforms, fan bulliforms, trichome hairs.

Source: Piperno, 2006; Rosen, 1992

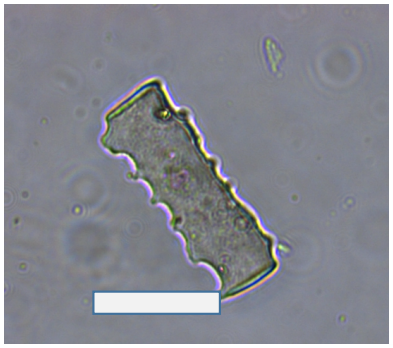

Parallelepiped thin sinuate elongate phytolith in MGD017 pellet. Scale bar is 20 microns.

Parallelepiped thin psilate elongate phytolith in MGD021. Scale bar is 20 microns.

Burnt multi-cell grass leaf/stem comprised of long-cells and a rondel phytolith in MGD017. Scale bar is 20 microns.

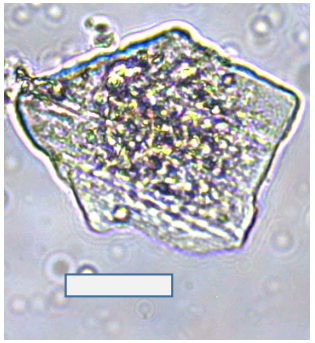

Multi-cell grass leaf/stem comprised of long-cells phytolith in MGD017. Scale bar is 20 microns.

Bulliform phytolith in MGD002. Scale bar is 20 microns.

Grass husk phytoliths

Morphotypes used for identification: single-cell and multi-cell papillae, long-cells echinate, long-cell dendritic/echinate/verrucate

Source: (Piperno, 2006; Rosen, 1992)

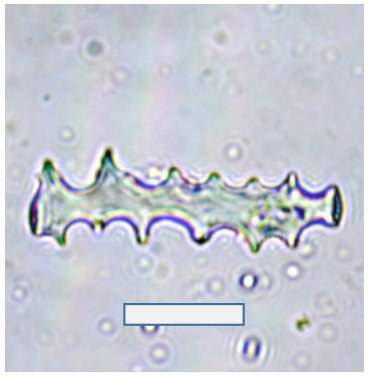

Single-cell long-cell dendritic in MGD021. Scale bar is 20 microns.

Single-cell long-cell dendritic in MGD001. Scale bar is 20 microns.

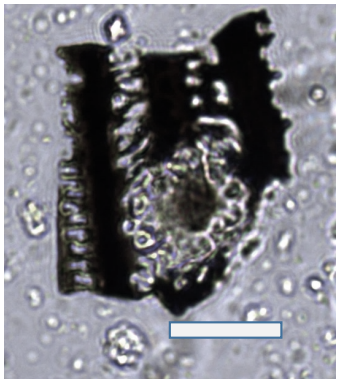

Burnt multi-cell long-cell dendritics with papilla in MGD001. Scale bar is 20 microns.

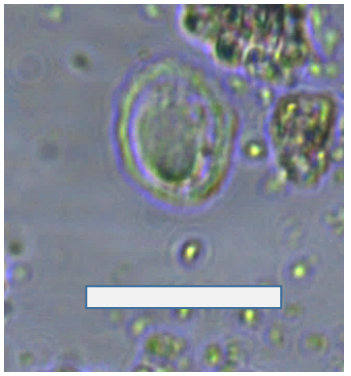

Single-cell papilla with papillae in MGD017. Scale bar is 20 microns.

Grass husk cf. wheat phytoliths

Morphotypes used for identification: multi-cell papillae, multi-cell long-cell echinate, multi-cell long-cell dendritic/echinate/verrucate

We identified cf. wheat with multi-cell dendritic long-cells with high rounded wave with irregular amplitude, variable papillae size range from 21–43 µm, with 16 to 18 pits, and a domed stippled surface and D-shaped cork cells. Most multi-cell husk phytoliths were not identified.

Source: (Rosen, 1992).

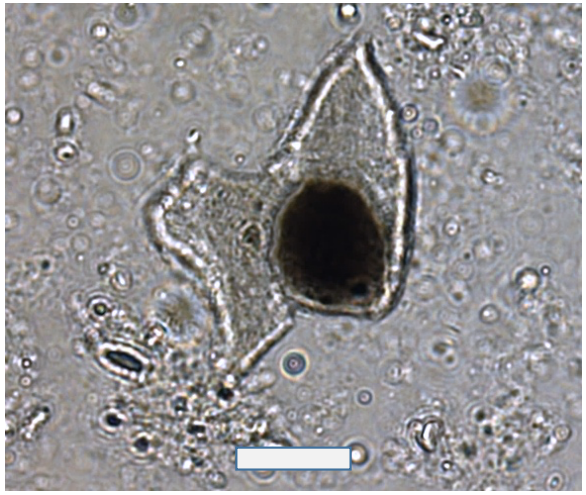

Multi-cell dendritic and papillae phytolith in MGD001. Scale bar is 20 microns

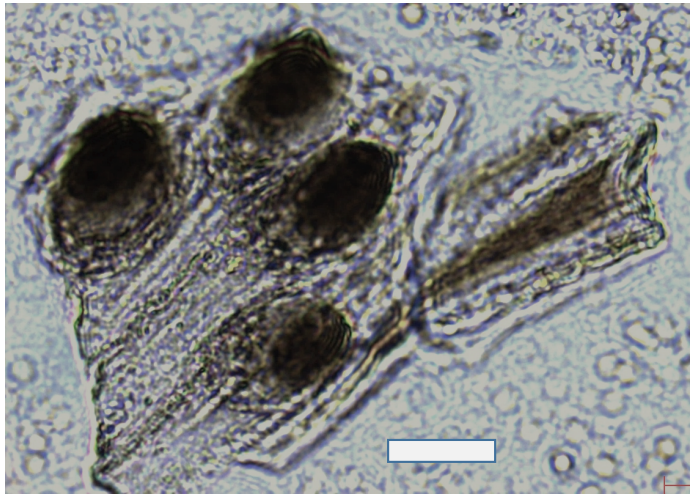

Multi-cell dendritic phytolith and papillae in MGD011. Scale bar is 20 microns

Unspecific parts of pooid (C3) grass phytoliths

Morphotypes used for identification: short-cell rondel, short-cell square trapezoid, short-cell oblong trapezoid

Source: (Piperno, 2006; Twiss et al., 1969)

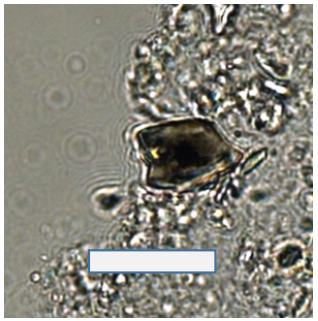

Short-cell rondel phytolith embedded in plaque matrix in MGD017. Scale bar is 20 microns.

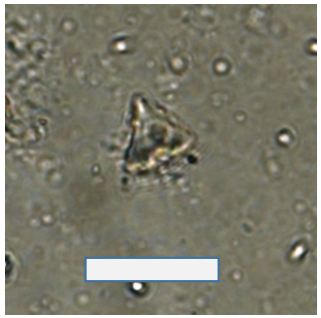

Short-cell rondel phytolith in MGD001. Scale bar is 20 microns.

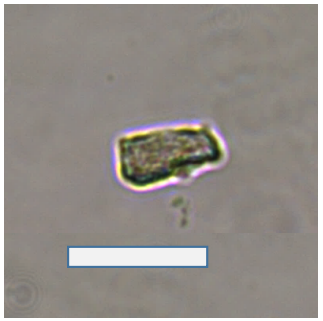

Short-cell trapezoid phytolith in MGD001. Scale bar is 20 microns.

Unspecific parts of chloridoid grass phytoliths

Morphotypes used for identification: short-cell saddle

Source: (Piperno, 2006; Twiss et al., 1969)

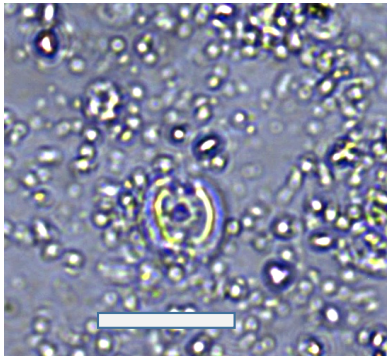

Short-cell saddle phytolith in MGD017 chunk. Scale bar is 20 microns.

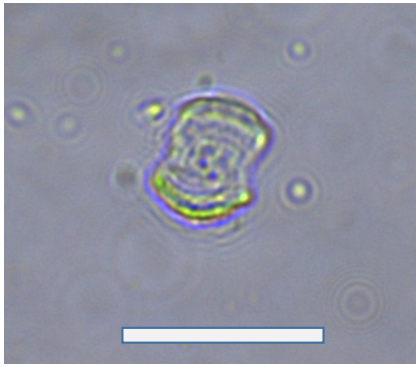

Short-cell saddle phytolith in MGD017 pellet. Scale bar is 20 microns.

Unspecific parts of (C4) grass phytoliths

Morphotypes used for identification: wide-lobed bilobates and short-cell crosses

We identified panicoid grasses using conventional grass short-cell conventions and we excluded short-cell flat bilobates due to the redundancy in grass tribes.

Source: (Rosen, 2006; Twiss et al., 1969)

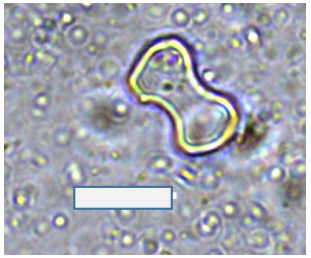

Wide lobed bilobate short-cell phytoliths in ERA017. Scale bar is 20 microns

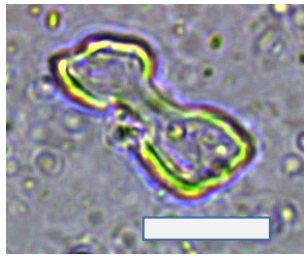

Wide lobed bilobate short-cell phytoliths in ERA017. Scale bar is 20 microns

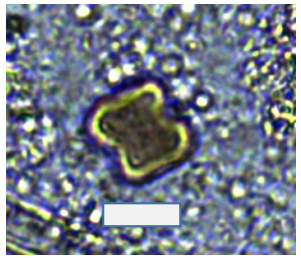

Cross short-cell in MGD011. Scale bar is 20 microns

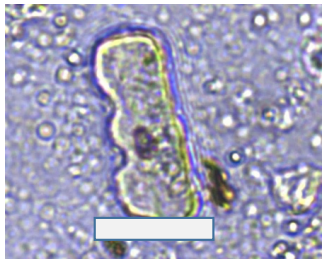

Polylobate short-cell in MGD001. Scale bar is 20 microns

Unspecific parts of panicoid millet type grass phytoliths

Morphotypes used for identification: wide-lobed bilobates

Source: (Out and Madella, 2016)

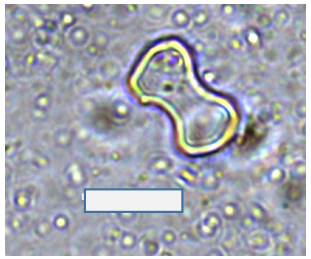

Wide lobed bilobate short-cell phytoliths in ERA017. Scale bar is 20 microns

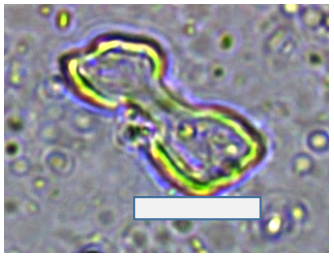

Wide lobed bilobate phytoliths short-cell in ERA017. Scale bar is 20 microns

Sedge leaf phytoliths

Morphotypes used for identification: Cones and hat shape

Source: (Pearsall and Dinan, 1992; Piperno, 2006)

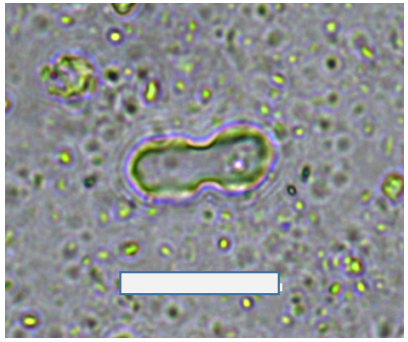

Sedge cones in ERA017. Scale bar is 20 microns

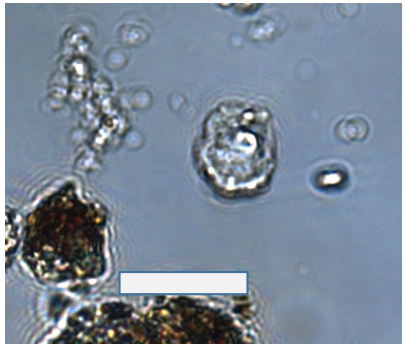

Sedge cones in MGD018. Scale bar is 20 microns

Date palms Phoenix sp. phytoliths

Morphotypes used for identification: spheroid echinate/ decorated and ovoid echinate/ decorated

5–12 microns diameter

Source: (Pearsall and Dinan, 1992; Piperno, 2006; Rosen, 1992)

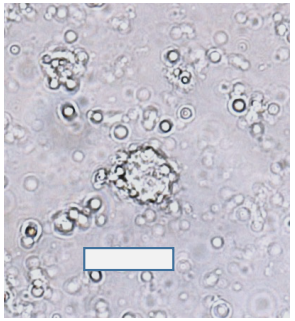

Date palm phytolith in MGD001. Scale bar is 20 microns

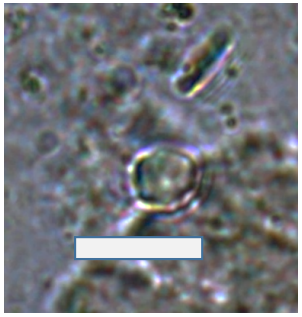

Date palm phytolith in MGD021. Scale bar is 20 microns

Unidentified palm taxon phytoliths (not date). Scale bar is 20 microns.

Morphotypes used for identification: spheroid echinate/decorated and ovoid echinate/decorated

Greater than 12 microns diameter

Source: (Pearsall and Dinan, 1992; Piperno, 2006; Rosen, 1992)

Ovoid echinate unidentified palm phytolith in MGD001. Scale bar is 20 microns.

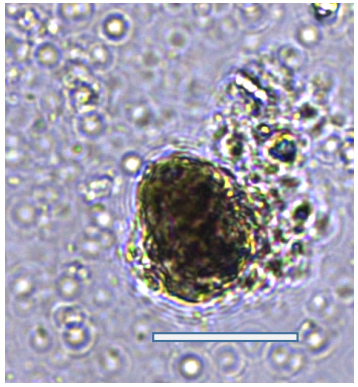

Ovoid echinate unidentified palm phytolith in MGD001. Scale bar is 20 microns.

Eudicot phytoliths

Morphotypes used for identification: plate, jigsaws, stomata cells, sulcate tracheary,

stomata tracheary, multi-cell polyhedral/spheroid/jigsaw

The broad category of eudicots can be identified with a number of phytoliths that form in aerial cellular structures particularly leaves, fruit and seeds and to a lesser extent bark, wood that have morphology that differs other plant groups. Other many of these structures occur in many eudicots, some eudicots poorly silicify.

Source: (Metcalfe and Chalk, 1950; Piperno, 2006, 1988)

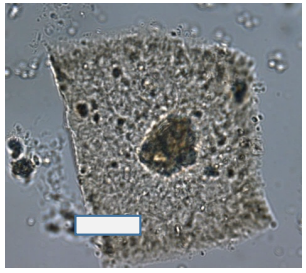

Plate phytolith in MGD002. Scale bar is 20 microns

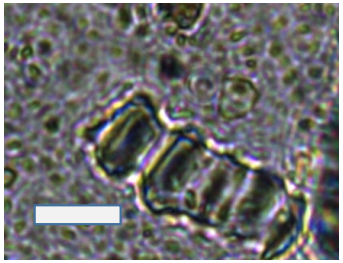

Sulcate tracheary phytolith in ERA017. Scale bar is 20 microns.

Tracheary phytolith in ERA017. Scale bar is 20 microns.

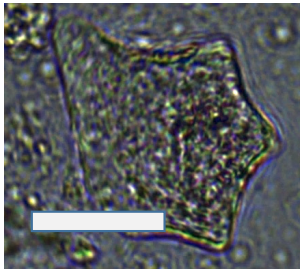

Polyhedral platey phytolith in MGD011. Scale bar is 20 microns.

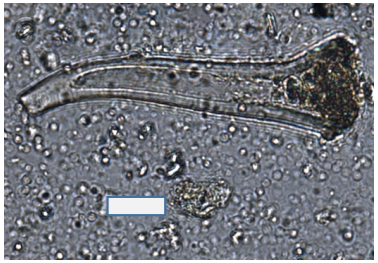

Dicot hair phytolith in MGD001. Scale bar is 20 microns.

Eudicot fruit phytoliths

Morphotypes used for identification: decorated jigsaws

Many eudicot phytoliths are highly nondiagnostic, partially due to

Source: (Albert et al. 2012; Metcalfe and Chalk, 1950; Piperno, 2006, 1988)

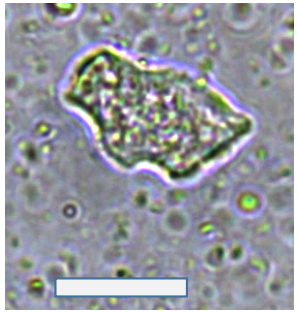

Jigsaw phytolith in MGD002.
Scale bar is 20 microns

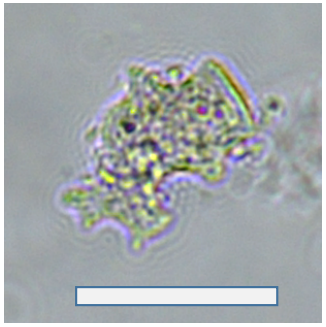

Jigsaw phytolith in MGD001.
Scale bar is 20 microns

Bark (angiosperm or gymnosperm) phytoliths

Morphotypes used for identification: spheroid psilate

Source: (Albert et al. 2012)

Two spheroid psilate phytoliths, possibly articulated in MGD001. Scale bar is 20 microns.

Phytoliths of unspecific plants

Morphotypes used for identification: hairs, parallelepiped thick elongate faceted, parallelepiped thin elongate curved, parallelepiped thick blocky elongate, parallelepiped thick elongate, parallelepiped thin blocky, parallelepiped thick blocky

Source: (Piperno, 2006; Twiss et al., 1969)

Parallelepiped thick block phytolith in MGD001. Scale bar is 20 microns.

Starches

Starches were detected using their translucent colour, the shape (spherical, globular, ovoid to polyhedral), surface features (lamellae rings, fissures, and hila), using the presence of birefringence crosses features under cross polarised light.

Source: (ICSN, 2011; Loy and Barton, 2006)

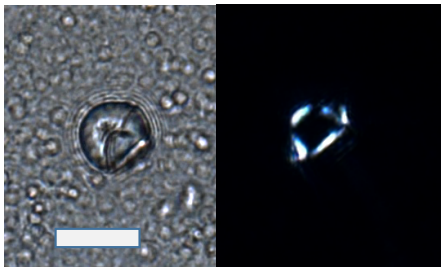

Nondiagnostic starch in MGD011, left brightfield, right cross polarisation. Scale bar is 20 microns.

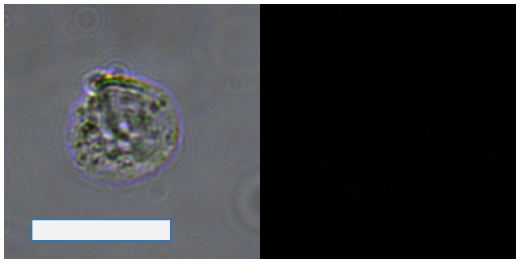

Damaged lenticular starch in MGD010 Triticeae (cereal), left brightfield, right cross polarisation. Scale bar is 20 microns. Starch is partially disrupted (via gelatinised heat treatment) and lacks birefringence

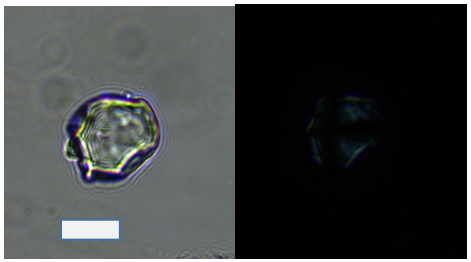

Unidentified polyhedral starch in MGD010. left brightfield, right cross polarisation. Scale bar is 20 microns.

Pollen

Pollen was distinguished from other microremains using standard protocols such as the presence of pores, color and surface texture and decoration and the lack of birefringence. Amongst pollens, only one type could be identified, a single Poaceae pollen using its monoporate surface, spherical like shape, smooth featureless surface, size, and clear color

Source: (Faegri et al., 1989)

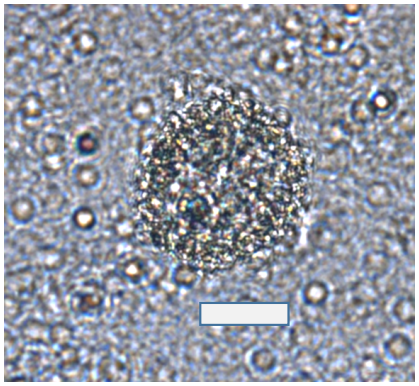

Damaged monoporate pollen from MGD011. Scale is 20 microns

Damaged triporate pollen from MGD001. Scale is 20 microns

Diatoms

Diatoms were identified from other particles using conventional features of diatom morphology. Diatoms were rare and sometimes damaged and we were not able to identify diatom to taxa

Source: (Juggins, 2001; Lacey and West, 2006)

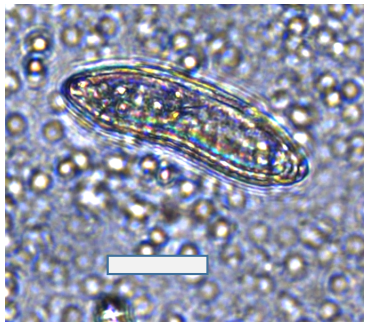

Pennate diatom in MGD011. Scale bar is 20 microns.

Pennate diatom in MGD017. Scale bar is 20 microns.

Sponge spicules

Sponge spicules were differentiated from other particles using colour, shape and surface texture

Damaged spicule from MGD001. Scale is 20 microns

Damaged spicule from MGD001. Scale is 20 microns

Fungal

Fungal particles were differentiated from other particles using colour, cell wall opacity, shape and surface texture

Source: (Lacey and West, 2006; Nilsson, 1985)

Fungal mycelium. Scale bar is 20 microns.

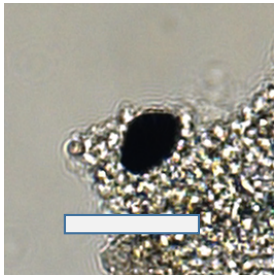

Unknown spore. Scale bar is 20 microns.

Unknown spore. Scale bar is 20 microns.

Unknown spore. Scale bar is 20 microns.

Charcoal

Fungal particles were differentiated from other particles using colour, cell wall opacity, shape and surface texture

Source: (Lacey and West, 2006; Nilsson, 1985)

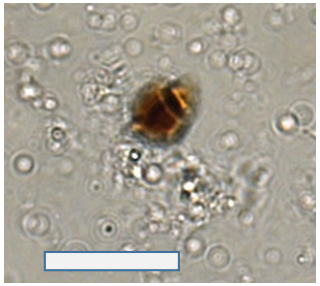

Charcoal fragment. Scale bar is 20 microns.

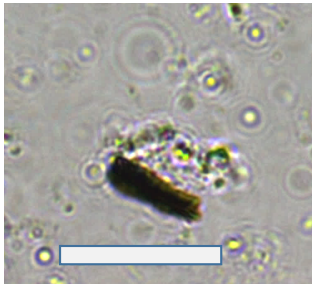

Charcoal fragment. Possible grass charcoal. Scale bar is 20 microns.

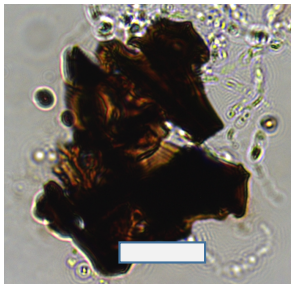

Unknown charcoal. Scale bar is 20 microns.

Invertebrates

Microscopic fragments of invertebrates were distinguished using cell shapes and they were classified into a invertebrate category.

Source: (Lacey and West, 2006)

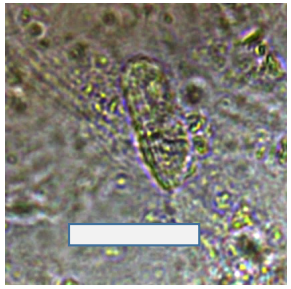

Fragmented invertebrate wing scale in MGD013. Scale bar is 20 microns.

Fibers, hairs and skin scales

Fibre were identified using their structure in brightfield and cross-polarised light. There were classified into several categories comprising of natural and artificial fibres and coloured or not coloured fibres. These likely derive from a mix of sources such as wood/paper, cotton and other natural fabric and synthetic fabrics.

Unsilicified plant fragments were rarely found but were occasionally recovered, and were distinguished from phytoliths due to texture, cross polarisation and colour.

Source: (Carr et al., 2008; Catling, 1981; Lacey and West, 2006; Körber-Grohne, 1988)

Plant fragment in MGD017 pellet. Scale bar is 20 microns.

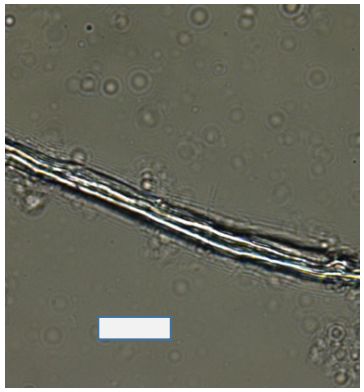

Natural fibre in MGD011. Scale bar is 20 microns.

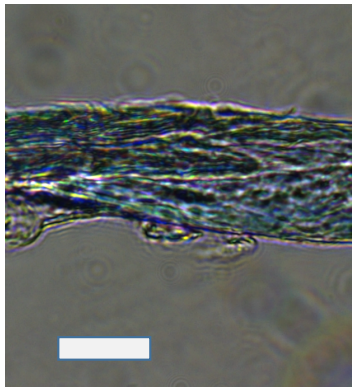

Natural fibre dyed blue in MGD011. Scale bar is 20 microns.

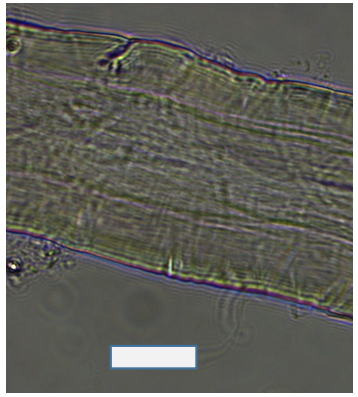

Mammal hair in MGD010. Scale bar is 20 microns.

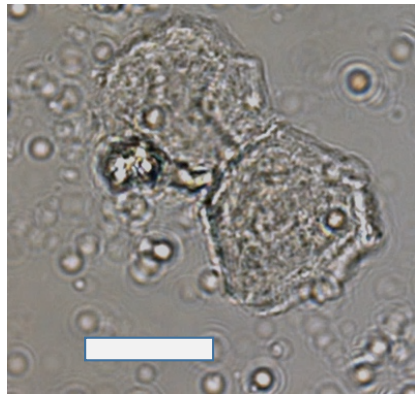

Skin scale in MGD006. Scale bar is 20 microns.

Unknown microremains

A variety of microremains, of different sizes, composed of siliceous, and other materials, probably relating to geological and biological origin, were found that could not be identified

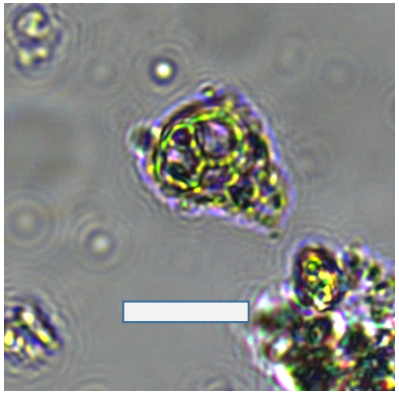

Unknown biogenic silica. Scale bar is 20 microns.

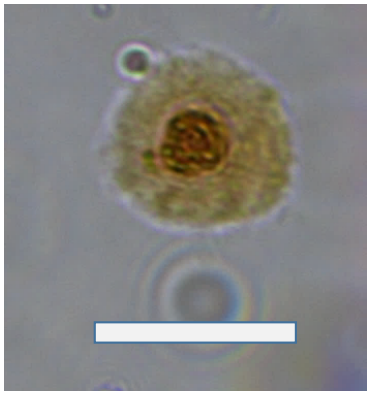

Unknown. Scale bar is 20 microns.

Unknown. Scale bar is 20 microns.

Bibliography

Albert, R.M. and Weiner, S., 2001. Study of phytoliths in prehistoric ash layers from Kebara and Tabun caves using a quantitative approach. Phytoliths: applications in earth sciences and human history, pp.251-266.

Albert, R.M., Berna, F. and Goldberg, P. 2012. Insights on Neanderthal fire use at Kebara Cave (Israel) through high resolution study of prehistoric combustion features: evidence from phytoliths and thin sections. Quaternary International 247 (2012): 278-293.

Boyadjian, C.H.C., Eggers, S., Reinhard, K., 2007. Dental wash: a problematic method for extracting microfossils from teeth. J. Archaeol. Sci. 34, 1622–1628.

Buckley, S., Usai, D., Jakob, T., Radini, A., Hardy, K., 2014. Dental calculus reveals unique insights into food items, cooking and plant processing in prehistoric central Sudan. PLoS One 9, e100808.

Carr, D., Cruthers, N., Smith, C., Myers, T., 2008. Identification of selected vegetable textile fibres. Stud. Conserv. 53, 75–87. https://doi.org/10.1179/sic.2008.53.supplement-2.75

Catling, D., 1981. Identification of Vegetable Fibres. Chapman and Hall, London.

Faegri, K., Kaland, P.E., Krzywinski, K., 1989. Textbook of pollen analysis. John Wiley & Sons Ltd, Chichester and New York.

Hardy, K., Radini, A., Buckley, S., Sarig, R., Copeland, L., Gopher, A., Barkai, R., 2015. Dental calculus reveals potential respiratory irritants and ingestion of essential plant-based nutrients at Lower Palaeolithic Qesem Cave Israel. Quat. Int. 398, 129–135. Hather, J.G., 2016. The identification of northern European woods: a guide for archaeologists and conservators. Routledge.

ICSN, 2011. The International Code for Starch Nomenclature [WWW Document]. URL http://fossilfarm.org/ICSN/Code.html (accessed 1.3.15).

Juggins, S., 2001. European diatom database.

Körber-Grohne, U., 1988. Microscopic methods for identification of plant fibres and animal hairs from the Prince's tomb of Hochdorf, Southwest Germany. J. Archaeol. Sci. 15, 73–82.

Lacey, M.E., West, J.S., 2006. The Air Spora - A Manual for Catching and Identifying Airborne Biological Particles, Plant Pathology. Springer-Verlag Gmbh, Dordrecht, the Netherlands

Lazzati, A.M.B., Levrini, L., Rampazzi, L., Dossi, C., Castelletti, L., Licata, M., Corti, C., 2015. The Diet of Three Medieval Individuals from Caravate (Varese, Italy). Combined Results of ICP-MS Analysis of Trace Elements and Phytolith Analysis Conducted on Their Dental Calculus. Int. J. Osteoarchaeol. https://doi.org/10.1002/oa.2458

Leonard, C.A., Vashro, L., O'Connell, J.F., Henry, A.G., 2015. Plant microremains in dental calculus as a record of plant consumption: a test with Twe forager-horticulturalists. J. Archaeol. Sci. Reports 2, 449–457. https://doi.org/10.1016/j.jasrep.2015.03.009

Loy, T., Barton, H., 2006. Post-excavation contamination and measures for prevention, in: Torrence, R., Barton, H. (Eds.), Ancient Starch Research. Left Coast Press, Walnut Creek, p. 165.

Metcalfe, C.R., Chalk, L., 1950. Anatomy of the dicots. The Clarendon Press, Oxford.

Nilsson, S., 1985. Atlas of airborne fungal spores in Europe. Springer, Berlin and Heidelberg. https://doi.org/10.1016/0048-9697(85)90178-0

Out, W.A., Madella, M., 2016. Morphometric distinction between bilobate phytoliths from Panicum miliaceum and Setaria italica leaves. Archaeol. Anthropol. Sci. 8, 505–521. https://doi.org/10.1007/s12520-015-0235-6

Pearsall, D.M., Dinan, E.H., 1992. Developing a phytolith classification system, in: George Rapp, J., Mulholland, S.C. (Eds.), Phytolith Systematics. Springer US, Boston, MA, pp. 37–64. https://doi.org/10.1007/978-1-4899-1155-1_3

Piperno, D.R., 2006. Phytoliths: A Comprehensive Guide for Archaeologists and Paleoecologists. AltaMira, Lanham.

Piperno, D.R., 1988. Phytolith analysis : an archaeological and geological perspective. Academic Press, San Digeo.

Power, R.C., Salazar-García, D.C., Wittig, R.M., Freiberg, M., Henry, A.G., 2015. Dental calculus evidence of Taï Forest Chimpanzee plant consumption and life history transitions. Sci. Rep. 5, 15161. https://doi.org/10.1038/srep15161

Power, R.C., Salazar-García, D.C., Wittig, R.M., Henry, A.G., 2014. Assessing use and suitability of scanning electron microscopy in the analysis of micro remains in dental calculus. J. Archaeol. Sci. 49, 160–169. https://doi.org/10.1016/j.jas.2014.04.016

Rosen, A.M., 1992. Preliminary Identification of Silica Skeletons from Near Eastern Archaeological Sites: An Anatomical Approach, in: Phytolith Systematics. Springer US, Boston, MA, pp. 129–147. https://doi.org/10.1007/978-1-4899-1155-1_7

Rosen, A.M., Weiner, S., 1994. Identifying ancient irrigation: a new method using opaline phytoliths from emmer wheat. J. Archaeol. Sci. 21, 125–132.

Tromp, M., 2012. Large-scale Analysis of Microfossils Extracted from Human Rapanui Dental Calculus: a Dual-Method Approach Using SEMEDS and Light Microscopy to Address Ancient Dietary Hypotheses. Idaho State University.

Tromp, M., Dudgeon, J. V, 2015. Differentiating dietary and non-dietary microfossils extracted from human dental calculus: the importance of sweet potato to ancient diet on Rapa Nui. J. Archaeol. Sci. 54, 54–63. https://doi.org/10.1016/j.jas.2014.11.024

Twiss, P.C., 1992. Predicted World Distribution of C3 and C4 Grass Phytoliths, in: Rapp, G., Mulholland, S.C. (Eds.), Phytolith Systematics. Springer US, Boston, MA, pp. 113–128. https://doi.org/10.1007/978-1-4899-1155-1_6

Twiss, P.C., Suess, E., Smith, R.M., 1969. Morphological Classification of Grass Phytoliths. Soil Sci. Am. Proc. 33, 109–115. https://doi.org/10.1007/s00702-011-0732-4

Warinner, C., Rodrigues, J.F.M., Vyas, R., Trachsel, C., Shved, N., Grossmann, J., Radini, A., Hancock, Y., Tito, R.Y., Fiddyment, S., Speller, C., Hendy, J., Charlton, S., Luder, H.U., Salazar-García, D.C., Eppler, E., Seiler, R., Hansen, L.H., Castruita, J.A.S., Barkow-Oesterreicher, S., Teoh, K.Y., Kelstrup, C.D., Olsen, J. V., Nanni, P., Kawai, T., Willerslev, E., von Mering, C., Lewis, C.M., Collins, M.J., Gilbert, M.T.P., Rühli, F., Cappellini, E., 2014. Pathogens and host immunity in the ancient human oral cavity. Nat. Genet. 46, 336–44. https://doi.org/10.1038/ng.2906